scientific reports

Check for updates

OPEN

TMBIM1 promotes epithelial mesenchymal transition by accelerating autophagic degradation of E-cadherin in glioblastoma

Lun Gao[1,2,3], Junhui Liu[1,2,3], Yong Li[1,2], Ji'an Yang[1,2], Jiayang Cai[1,2], Long Wang[1,2], Zhang Ye[1,2], Shi'ao Tong[1,2], Gang Deng[1,2]✉, Qianxue Chen[1]✉ & Qiang Cai[1]✉

Glioblastoma (GBM; WHO grade IV) is well known for its highly aggressive and recurrent nature and accounts for approximately 50% of all gliomas. Dysregulation of epithelial–mesenchymal transition (EMT) can lead to malignant progression of GBM. Therefore, it is an urgent need to delineate the mechanisms by which molecular drivers affect EMT in GBM. We found for the first time that transmembrane BAX inhibitor motif-containing 1 (TMBIM1) was overexpressed in GBM tissues compared with nontumor brain tissues and that its expression level was correlated with the degree of malignancy of glioma. Patients with high TMBIM1 expression had shorter overall survival times than those with low TMBIM1 expression. Importantly, TMBIM1 induced EMT and autophagy, and inhibition of autophagy reversed TMBIM1-induced EMT in both in vitro and in vivo assays. TMBIM1 induced EMT by downregulating E-cadherin expression, which mediated by in-habitation of autophagic degradation of E-cadherin. Inhibition of TMBIM1 expression dramatically decreased the levels of p-AMPKα Thr172 and p-ULK1 Ser317 in U87 and U251 cells and increased the level of p-mTOR Ser2448. In addition, inhibition of AMPK (adenosine monophosphate-activated protein kinase)/mTOR (mammalian target of rapamycin)/ULK1 (unc-51–like autophagy-activating kinase 1) axis partially attenuated TMBIM1-induced autophagy. Our study provides a novel mechanism for the regulation of EMT in the process of GBM invasion and migration, indicating that suppression of TMBIM1 activity to attenuate autophagy may be a potential strategy for the treatment of GBM.

Keywords TMBIM1, Glioblastoma, Epithelial-mesenchymal transition, Autophagy, AMPK-mTOR-ULK1 axis

Abbreviations

GBM	Glioblastoma
TMBIM1	Transmembrane BAX inhibitor motif-containing 1
CHX	Cycloheximide
CQ	Chloroquine
EMT	Epithelial-mesenchymal transition
LGG	Lower-grade gliomas
IHC	Immunohistochemistry
TCGA	The Cancer Genome Atlas
CGGA	Chinese Glioma Genome Atlas
IDH	Isocitrate dehydrogenase
WT	Wild type
NBT	Normal brain tissue
AMPK	Adenosine monophosphate-activated protein kinase

[1]Department of Neurosurgery, Renmin Hospital of Wuhan University, Wuhan 430060, China. [2]Central Laboratory, Renmin Hospital of Wuhan University, Wuhan 430060, China. [3]Lun Gao and Junhui Liu contributed equally to this work. ✉email: gang.deng@whu.edu.cn; chenqx666@whu.edu.cn; caiqno@whu.edu.cn

mTOR	Mammalian target of rapamycin
ULK1	Unc-51–like autophagy-activating kinase 1
TEM	Transmission electron microscopy

Glioma is the most common primary intracranial tumor in adults, accounting for more than 70% of malignant brain tumors, among which GBM is the most malignant[1,2]. However, despite the combination therapeutic regimen of tumor resection, radiotherapy and chemotherapy, the median survival time of GBM is only 12–18 months, and the 5-year survival rate is less than 5%[3]. GBM is notorious for its high invasiveness and recurrence ability, which may be the key reason that the treatment of GBM is medically unsatisfactory[4]. Therefore, exploring the molecular mechanisms underlying the highly invasive capacity of GBM may contribute to improving patient outcomes.

Epithelial-mesenchymal transition (EMT) allows epithelial cells to acquire mesenchymal characteristics and enhances metastasis and invasion[5]. Studies have shown that EMT is considered to be the main driving force of tumor progression and plays a vital role in promoting tumor recurrence, metastasis and chemotherapeutic resistance[6]. Autophagy is a conserved cellular process involved in the degradation and recycling of cellular components. Autophagy directly regulates GBM cell function by regulating cell proliferation, migration and invasion, and indirectly by affecting the GBM tumor microenvironment (such as immune cell population and tumor metabolism)[7]. Loss of E-cadherin during cancer progression is fundamental to the activation of EMT, and autophagic degradation of E-cadherin is an important contributor to this process[8]. Sphingosine kinase 1 (SPHK1) is a regulator of sphingolipid metabolites that induces EMT in hepatoma cells by accelerating lysosomal degradation of E-cadherin. Moreover, overexpression of SPHK1 leads to the interaction between tumor necrosis factor-associated factor 1 (TRAF1) and BECN1, which activates lysine ubiquitination of BECN by promoting autophagy[9]. Currently, the role of the autophagy-lysosomal degradation pathway in regulating the EMT process has been extensively studied in cancers, including glioma[10,11].

TMBIM1 is a membrane protein that is localized in endosomes/lysosomes and plays crucial roles in vascular remodeling and mediating cystic medial degeneration[12]. TMBIM1 is associated with regulating cell apoptosis and maintaining intracellular calcium homeostasis[13]. TMBIM1 expression is elevated in colorectal cancer tissues, and genetic alteration of TMBIM1 is associated with a high risk of lymph node metastasis and distant metastasis[14]. Hongliang Li reported that TMBIM1 inhibits adipocyte proliferation and ameliorates obesity-related metabolic diseases by promoting lysosomal degradation of Toll-like receptor 4 (TLR4)[15,16]. Lysosomal degradation is a fundamental self-digestion process occurring during autophagy. Impairment of the autophagy-lysosomal degradation pathway has been associated with cancer.

Considering the importance of TMBIM1 in regulating the autophagy-lysosomal pathway, we tried to find the potential mechanism by which TMBIM1 regulates the EMT process in GBM. In our study, we demonstrated that TMBIM1 was overexpressed in GBM and that high TMBIM1 expression predicted poor prognosis in GBM and lower-grade glioma (LGG; WHO grade II-III). Moreover, our research showed that TMBIM1 induced autophagy and EMT-mediated cell invasion and migration. Subsequent studies confirmed that TMBIM1 regulates autophagy in GBM through the AMPK/mTOR/ULK1 axis, and inhibiting autophagy partially reversed the EMT induced by TMBIM1.

Materials and methods

Bioinformatics

A total of five glioma datasets were obtained from the GlioVis portal (http://gliovis.bioinfo.cnio.es)[17]: the TCG A-GBM, TCGA-GBMLGG, CGGA, Rembrandt and Gravendeel datasets.

Human tissue samples

The paraffin-embedded glioma tissue microarray contained 111 glioma tissues and 8 normal brain tissues. All tissue samples were obtained in the Department of Neurosurgery, Renmin Hospital of Wuhan University between March 2016 and June 2019. Details of the clinical information of all patients are presented in Table 1. The other 5 nontumor brain tissues (NBT) and 18 GBM tissues were collected between March 2019 and March 2021 for Western blot (WB) analysis. All NBTs were obtained from patients with severe brain injury who needed surgery. None of the patients received radiotherapy or chemotherapy before surgery, and all tissues were stored in liquid nitrogen. This study was approved by the Ethics Committee of the Renmin Hospital of Wuhan University [approval number: 2012LKSZ (010) H], and all procedures were conducted in accordance with the Helsinki Declaration and all the patients signed the informed consent form.

Antibodies and reagents

CHX (S7418), MG132 (S2619), Compound C (S7306), CQ (S6999) and 3-MA (HY-19312) were purchased from Selleck. Antibodies specific for E-cadherin (20874-1-AP), N-cadherin (22018-1-AP), Vimentin (10366–1-AP), SNAI1 (13099-1-AP), P62 (18420–1-AP), Beclin1 (11306-1-AP), AMPK (66536-1-Ig) and ULK1 (20986-1-AP) were obtained from Proteintech (Wuhan, China). Anti-Flag (ANT301) and anti-β-actin (ANT321) antibodies were purchased from AntGene (Wuhan, China). Anti-phospho-AMPKα (Thr172) (#2535), anti-phospho-ULK1 (Ser317) (#12753) and anti-phospho-mTOR (Ser2448) (#5536) antibodies were obtained from Cell Signaling Technology (USA). The anti-LC3 antibody (GB11124) was purchased from Servicebio (Wuhan, China).

Cell culture and transfection

The U87 (U87-MG ATCC, CVCL_0022) and U251 cell lines were purchased from the Cell Bank of the Chinese Academy of Sciences (Shanghai, China). All cell lines were identified by STR profiling by Procell Life Science & Technology Co., Ltd. (Wuhan, China). Proof of cell line identification is provided in the supplementary

Variables	Number	TMBIM1 expression		Chi-square value	P value
		Low	High		
Age (years)				1.302	0.254
< 60	89	36	53		
≥ 60	22	6	16		
Gender				0.181	0.671
Female	50	20	30		
Male	61	22	39		
Location				0.0219	0.883
Supratentorial	101	38	63		
Subtentorial	10	4	6		
KPS				1.551	0.213
≥ 80	74	31	43		
< 80	37	11	26		
Grade				4.015	0.045
LGG	66	30	36		
GBM	45	12	33		

Table 1. Association between TMBIM1and clinical features.

material. Cells were cultured in Dulbecco's modified Eagle's medium (DMEM) supplemented with 10% fetal bovine serum (FBS) (Gibco, USA). All cells were cultured at 37 °C in a humidified atmosphere of 5% CO2. The Flag-TMBIM1 and vector control plasmids were obtained from Miaolingbio (Wuhan, China). Transfection was performed when the cells reached a fusion degree of about 70%. 2ug of plasmid and 5ul of Hieff Trans™ Liposomal Transfection Reagent (Yeasen Biotechnology, China) were added to each well of the 6-well plate. Fresh medium was added after transfection for 6 h, and cells were transfected for 48 h for follow-up experiments.

Establishment of stable cell lines

The lentiviral vector for TMBIM1 knockdown (rLV-shRNA-TMBIM1) was obtained from Huamengbio (Wuhan, China), and all lentiviral vectors were verified by DNA sequencing. Cells were cultured in 6-well plates and infected with lentivirus according to the manufacturer's instructions for 24 h. Subsequently, the cells were treated using puromycin (2 μg/ml) for 72 h, and fresh medium was added after washing with PBS buffer. The knockdown efficiency of TMBIM1 was verified by real-time qPCR and WB analyses. The TMBIM1 shRNA sequences were as follows: shTMBIM1-1-F: 5′GATCCGGAGAGAGCGGTGAGTGATAGCTCGAGCTATCAC TCACCGCTCTCTCCTTTTTTG-3′, shTMBIM1-1-R: 5′-AATTCAAAAAAGGAGAGAGCGGTGAGTGATA GCTCGAGCTATCACTCACCGCTCTCTCCG-3′, shTMBIM1-2-F: 5′-GATCCGCCGTTTCCCATGGAACA TCACTCGAGTGATGTTCCATGGGAAACGGCTTTTTTG-3′, shTMBIM1-2-R: 5′-AATTCAAAAAAGCCG TTTCCCATGGAACATCACTCGAGTGATGTTCCATGGGAAACGGCG-3′.

Transwell assays

Cell invasion and migration were evaluated using Transwell inserts with and without a Matrigel (R&D, USA) coating, respectively. A total of 3×10^5 cells in serum-free medium were added to the upper chamber, and 600 μl of DMEM supplemented with 10% FBS was added to the lower chamber. The cells were fixed with 4% paraformaldehyde for 30 min after incubation in an incubator (37 °C, 5% CO2) for 24 h. Then, the cells were stained with 0.5% crystal violet for 15 min and observed under a microscope (Olympus, BX51, Japan). In each experimental group, we randomly selected 6 fields to calculate the average cell count, and we repeated all the experiments three times.

Western blot analysis

Cells were lysed in RIPA lysis buffer (Beyotime, China) on ice for approximately 30 min after 3 washes with PBS buffer. After centrifugation, SDS-PAGE sample loading buffer was added to the protein lysates and heated at 100 °C for 10 min. Equal amounts of protein were loaded into SDS-PAGE gels and then transferred to PVDF membranes. After blocking in buffer containing 5% skim milk powder for 60 min, the membranes were incubated with the primary antibody at 4 °C overnight. The next day, the membranes were incubated with the secondary antibody after washing with PBST, and bands were then visualized using a ChemiDoc™ Touch Imaging System (Bio–Rad, China).

RNA isolation and RT–PCR

Total RNA was extracted from cells by using TRIzol reagent (Invitrogen, USA). A PrimeScript RT Reagent Kit with gDNA Eraser (RR047A, Japan) was used to synthesize cDNA. Quantitative RT-PCR was performed using SYBR® Premix Ex Taq™ II (RR820A, Takara). The specific primer pairs were as follows: GAPDH Forward: 5′-TGCCAAATATGATGACATCAAGAA-3′, GAPDH Reverse: 5′-GGAGTGGGTGTCGCTGTTG-3′. TMBIM1 Forward: 5′-CACCCGATGCCCATGAACTA-3′, TMBIM1 Reverse: 5′-CACTTTCCGGTCATCCCACT-3′,

E-cadherin Forward: 5′-GCGAACTGTTTGCAGAGG-3′, E-cadherin Reverse: 5′-CAGTGCGTGTCGTGGAGT-3′

Immunohistochemistry

Normal brain and glioma tissues were embedded in paraffin and sectioned. The sections were deparaffinized with xylene for 15 min and then dehydrated sequentially with 100%, 95% and 75% ethanol. After washing with PBS buffer three times, Tris–EDTA antigen repair solution (Servicebio, China) was used for antigen retrieval, and endogenous peroxidase activity was quenched with 3% H_2O_2. Subsequently, the sections were incubated with the primary antibody overnight and the HRP-labeled secondary antibody (Service bio, China) for 1 h the next day. DAB staining solution (Service bio, China) was added to the sections, which were also stained with hematoxylin. The intensity of IHC staining was scored as 0, 1, 2, and 3 points, which indicated background staining, faint staining, moderate staining and strong staining, respectively. Two independent pathologists examined and scored the samples. If the pathologists had different opinions, staining was also scored by a third pathologist. Samples with an IHC score of 0–1 were classified into the low expression group, and those with a score of 2–3 were classified into the high expression group.

Autophagosome and autophagic flux detection

For electron microscopy analysis, cells were collected in a 1.5 ml EP tube. The cells were fixed with cold fixative solution (Servicebio, China) overnight at 4 °C and were then embedded, sectioned and observed by transmission electron microscopy (TEM) (Hitachi, Japan). Lenti-mCherry-EGFP-LC3B lentivirus (Beyotime, China) was used for monitoring autophagic flux in U251 cells transfected with the vector or Flag-TMBIM1 plasmid for 24 h. After infection for 24 h, the cells were fixed with 4% paraformaldehyde and observed and photographed with a confocal fluorescence microscope (FV1200, Olympus).

Intracranial xenograft model

BALB/c-nu mice purchased from Shaulaibao Biotechnology Co., Ltd (Wuhan, China) were fed adaptively in SPF environment for one week. U87 cells transduced with sh-TMBIM1 or the control shRNA were harvested by trypsinization, washed with PBS, and resuspended at a concentration of 1×10^5 cells/μl; then, 4×10^5 cells were injected into the right striata of 6-week-old BALB/c nude mice. The sh-TMBIM1 cell-injected mice were randomly divided into two groups (n = 10), and CQ (50 mg/kg) or DMSO was injected every 2 days for a total of 10 injections beginning 10 days after cell inoculation. Tumor volume was monitored by bioluminescence using an IVIS 200 Spectrum Imaging System (Caliper Life Sciences, USA) after retroorbital injection of luciferin (150 mg/kg). For survival analysis, we observed nude mice on a regular basis and euthanized their cervical vertebrae after anesthesia by inhalation of isoflurane (Raymarching) when severe neurological symptoms and/or significant weight loss (more than 20% of initial body weight) occurred.Then, the brain tissue of the nude mice was removed, fixed with polyoxymethylene, and embedded in paraffin. The animal experiment was reviewed and approved by the Animal Ethics Committee of Renmin Hospital of Wuhan University [approval number: WDRM 20201111]. All methods were carried out in accordance with ARRIVE guidelines. All methods were performed in accordance with the relevant guidelines and regulations.

Statistical analysis

The results are presented as the means ± standard deviations. Unpaired student's t test was used to analyze differences between two groups. For comparisons among three or more groups, one-way analysis of variance (ANOVA) was used, and Tukey's multiple comparisons test was performed to analyze differences between groups when the results of analysis of variance indicated a significant difference. Patients were divided into high and low expression groups with the upper quartile value as the cutoff, and Kaplan–Meier survival analysis was used to determine the significance of differences between the groups. This analysis was performed with GraphPad Prism 8.0 software. SP33.23 software was used to perform univariate and multivariate Cox regression analyses. A p value < 0.05 was considered significant.

Results

TMBIM1 is overexpressed in GBM

To compare the expression of TMBIM1 between GBM and normal brain tissues (NBTs), normalized RNA-Seq data from TCGA and Rembrandt datasets were used. The results indicated that TMBIM1 expression was elevated in GBM tissues compared to normal brain tissues (Fig. 1A). To further explore the expression pattern of TMBIM1 in GBM, Western blot and immunohistochemical (IHC) analyses were conducted on the in-house cohort. The results further proved that the expression level of TMBIM1 in GBM tissues was higher than that in NBTs (Fig. 1B–E).

TMBIM1 expression correlated with malignancy and predicted worse prognosis in gliomas

The WHO classifies gliomas as grades II-IV according to the degree of malignancy[18]. We demonstrated that TMBIM1 expression was higher in grade IV compared with grade II–III in The Cancer Genome Atlas (TCGA), the Chinese Glioma Genome Atlas (CGGA), and the Rembrandt and Gravendeel datasets (Fig. 2A), and we showed that TMBIM1 expression was higher in GBM tissues than in LGG tissues by IHC staining analysis in the in-house cohort (Fig. 2B, C). Testing for two mutations (IDH1/2 mutations and 1p19q codeletion) has been widely used in the diagnosis and classification of glioma[18]. In TCGA and CGGA, TMBIM1 expression was generally higher in GBM patients with wild-type isocitrate dehydrogenase (IDH)1/2 (IDH-wt). We found that regardless of the presence of 1p19q was codeletion, TMBIM1 expression was increased in LGG patients with wild-type IDH 1/2 compared with those with IDH ½ mutation (IDH-mut) (Fig. 2D–F). Then, we explored the association

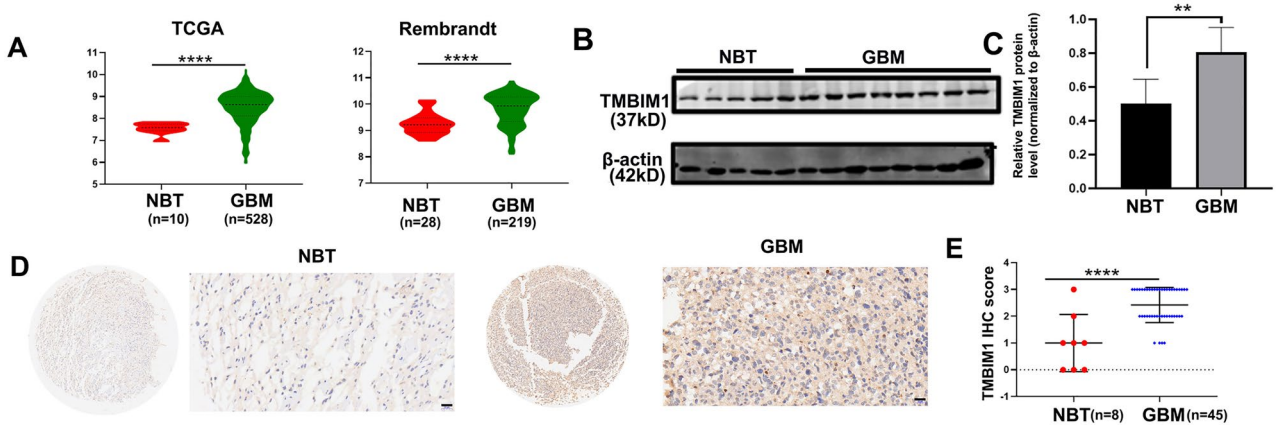

Fig. 1. TMBIM1 is overexpressed in GBM. (**A**) Analysis of TMBIM1 mRNA expression in normal brain tissues (NBT) and GBM tissues in TCGA and Rembrandt datasets. (**B, C**) TMBIM1 expression in normal brain tissues and GBM tissues. (**D**) Representative images of IHC staining of TMBIM1 in NBT and GBM tissues. Scale bars, 20 um. (**E**) IHC score of NBTs and GBM tissues in our independent cohort. Unpaired student t-test was used to measure statistical significance in NBT group and GBM group * $P < 0.05$, *** $P < 0.0001$.

between TMBIM1 expression and clinical prognosis. Kaplan–Meier analysis was performed to determine the prognostic role of TMBIM1 in LGG, GBM and overall glioma, and the results demonstrated that high TMBIM1 expression predicted worse prognosis in the TCGA, CGGA, and Gravendeel datasets (Fig. 2G, Fig. S1A, S1B). To examine independent risk factors for poor prognosis in glioma patients, we performed multivariable Cox proportional hazards regression analysis. The results showed that TMBIM1 was an independent risk factor for prognosis in glioma in the TCGA and CGGA datasets (Table S1, S2). These results indicated that TMBIM1 might be a novel oncogene and prognostic marker in glioma.

TMBIM1 promotes EMT in GBM cells

GBM was subclassified into four subtypes by Verhaak et al.: classical, mesenchymal, neural and proneural[19]. GBM with the mesenchymal subtype is considered to have significant metastatic ability and poor prognosis. We found that TMBIM1 expression was higher in the mesenchymal subtype (Fig. S2A). Loss of E-cadherin protein expression is considered to be the basis of EMT, which is related to an increase in cell metastasis[9]. As expected, E-cadherin expression was negatively correlated with TMBIM1 expression, as determined by IHC staining (Fig. 3A, B). TMBIM1 mRNA expression was positively correlated with that of mesenchymal markers such as SNAI1 and vimentin (VIM), based on the CGGA dataset (Fig. S2B). Then, we investigated whether TMBIM1 can enhance the invasion and migration potential of GBM cells by regulating EMT. The results revealed that knockdown of TMBIM1 expression inhibited the migration and invasion of U251 and U87 cells (Figs. 3C–E; S2C–S2E) and that overexpression of TMBIM1 facilitated cell migration and invasion (Figs. 3D, F; S2D–S2F). We also found that TMBIM1 knockdown increased the expression of the epithelial marker E-cadherin and decreased the expression of mesenchymal markers such as Vimentin, N-cadherin and SNAI1. Furthermore, overexpression of TMBIM1 resulted in increased expression of Vimentin, N-cadherin and SNAI1 and a slight decrease in E-cadherin expression (Figs. 3G, S2G–2J). We evaluated the expression of markers of EMT in GBM tissues by Western blotting. The results demonstrated that the protein level of TMBIM1 was negatively correlated with that of E-cadherin and positively correlated with those of N-cadherin and SNAI1 (Figs. 3H, S2K). These results revealed that TMBIM1 can induce EMT in GBM cells.

TMBIM1 stimulates autophagy in GBM cells

Previous studies have identified TMBIM1 as a lysosomal transmembrane protein[15], and we speculated that TMBIM1 might be involved in the regulation of autophagy. Beclin1 can mediate the localization of autophagic proteins to phagophores and regulate the formation and maturation of mammalian autophagosomes[20]. At present, it is widely believed that p62 is the effector molecule and the substrate of selective autophagy. p62 binds to ubiquitinated proteins and then forms complexes with LC3-II proteins that are localized on autophagic membranes and degraded in autolysosomes[21]. LC3 is protein light chain 3, which is a marker of autophagy. LC3 is mainly involved in the formation of autophagosomes. There are four types of LC3 isomers in mammals (LC3A, LC3B, and LC3C). LC3 precursor molecules undergo proteolysis mediated by ATG4B to remove the C-terminal 5-peptide and cleaved to generate the cytoplasmic form LC3-I. LC3-I is then activated by APG7L/ATG7, transferred to ATG3 and conjugated to form the membrane-binding protein LC3-II, which is attached to the autophagosome membrane. It is clear that the occurrence of LC3B-II is crucial in the process of autophagy, and LC3B is widely used to detect autophagy in various cell types[22–24]. Therefore, Beclin1, p62 and LC3 are commonly used to investigate autophagy. We found by IHC staining of a tissue microarray that TMBIM1 expression was positively correlated with Beclin1 expression (Fig. 4A, B). The Western blot results indicated that TMBIM1 expression was positively correlated with Beclin1 expression and negatively correlated with p62 expression in GBM tissues (Figs. 4C, S3A). In addition, TMBIM1 overexpression increased the protein levels

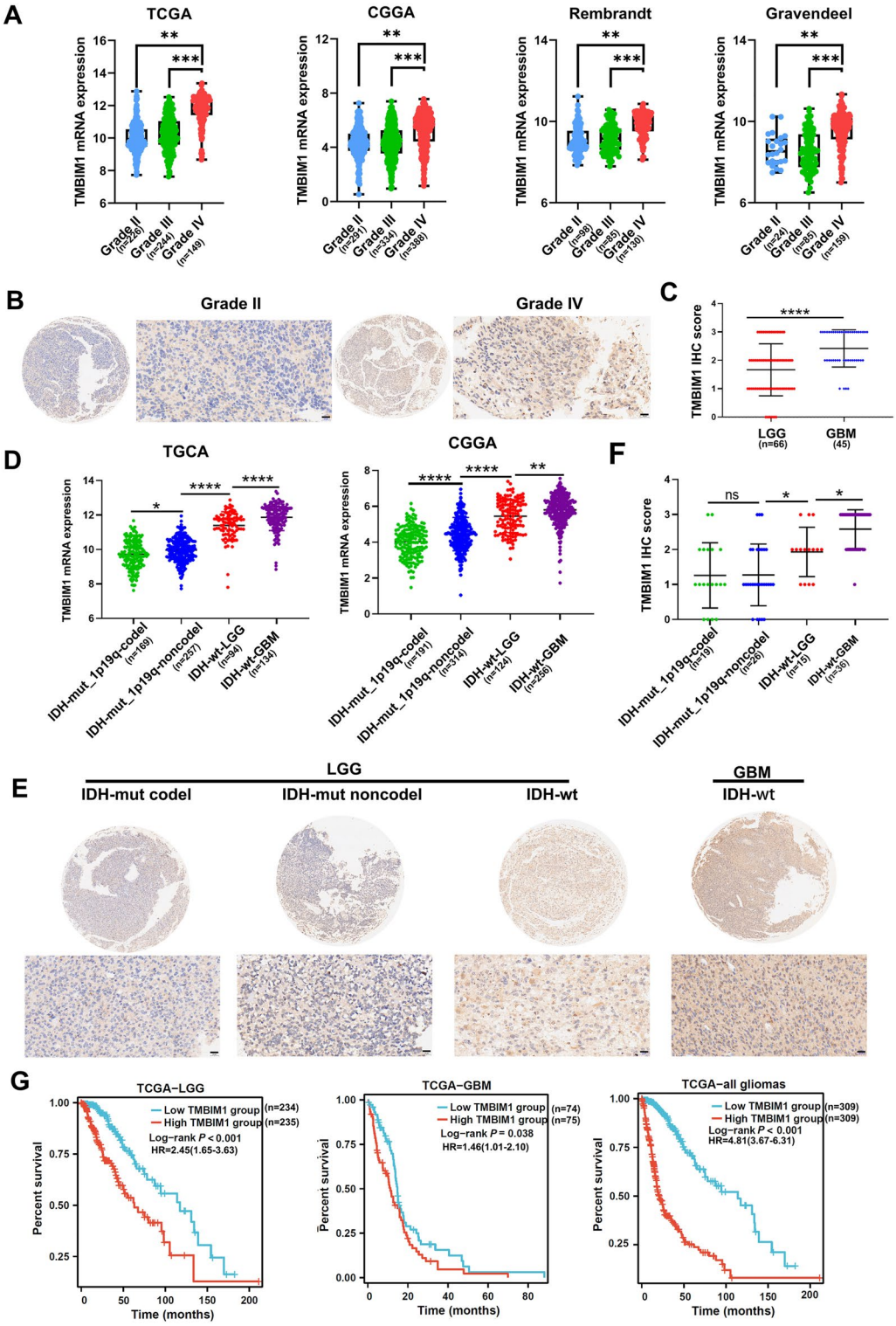

Fig. 2. TMBIM1 expression correlated with malignancy and predicted worse prognosis in gliomas. (**A**) TMBIM1 mRNA expression level in gliomas of different WHO grades based on the TCGA, CGGA, Rembrandt and Gravendeel datasets. (**B, C**) IHC staining of TMBIM1 in glioma tissues. Scale bars, 20 um. (**D**) TMBIM1 expression in gliomas with different IDH and 1p19q statuses in the TCGA and CCGA datasets. (**E, F**) IHC analysis of TMBIM1 expression in glioma tissues with different IDH and 1p19q statuses. Scale bars, 20um. (**G**) Kaplan–Meier survival analysis based on TMBIM1 expression in our in-house cohort. Unpaired student t-test was used to analyze differences between two groups. For comparisons among three or more groups, one-way analysis of variance (ANOVA) was used, and Tukey's multiple comparisons test was performed to analyze differences .* $P < 0.05$; ** $P < 0.01$; *** $P < 0.001$; **** $P < 0.0001$; ns, nonsignificant; mut, mutant; wt; wild-type; HR, Hazard Ratio.

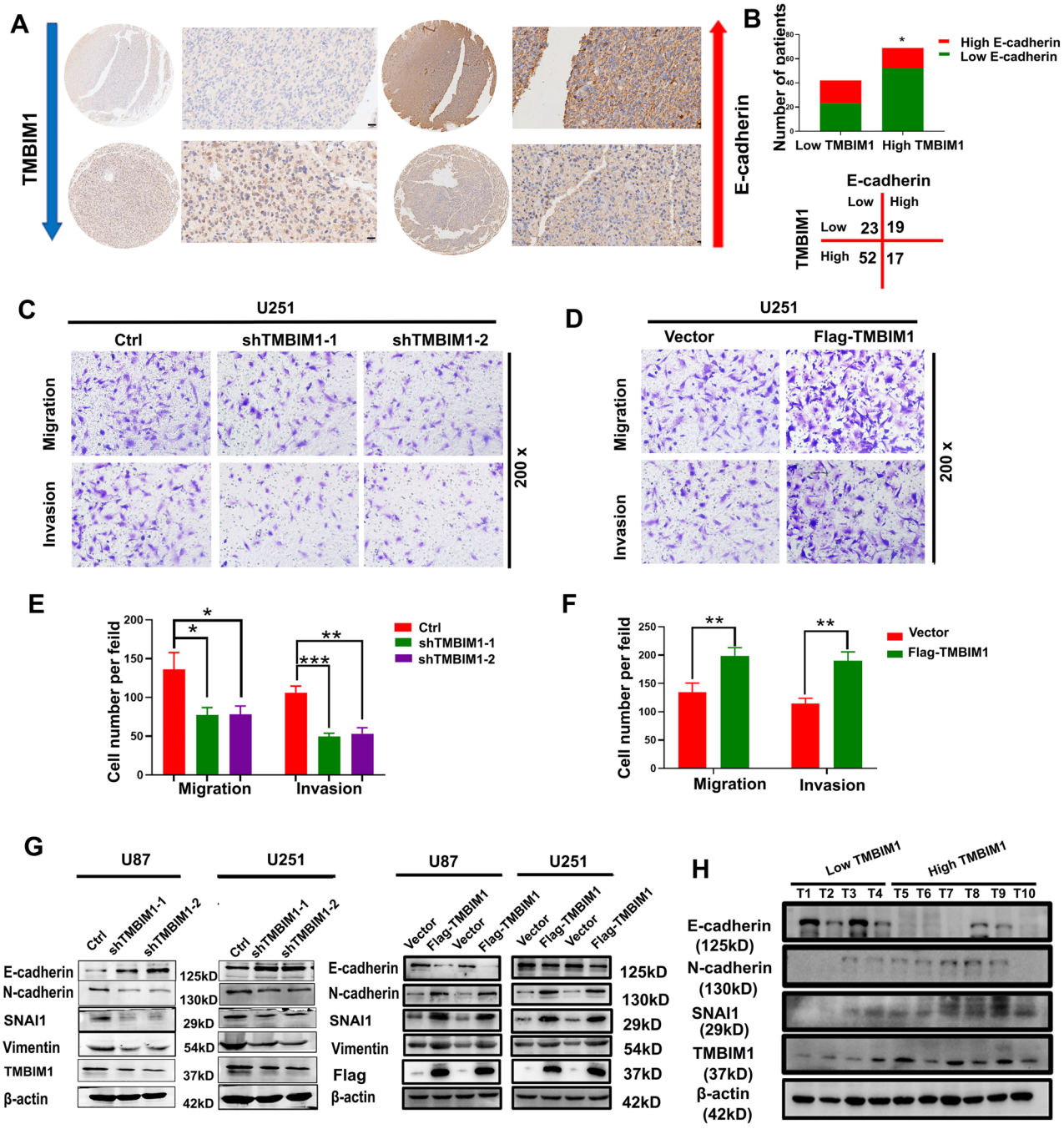

Fig. 3. TMBIM1 promotes EMT in GBM cells. (**A**) Representative images of IHC staining showing that TMBIM1 expression was negatively correlated with E-cadherin expression in the same tissues. Scale bars, 20um. (**B**) The expression of TMBIM1 and E-cadherin in 111 glioma samples was analyzed. (**C**). TMBIM1 knockdown inhibited the migration and invasion of U251 cells. (**D**) TMBIM1 overexpression enhanced the migration and invasion of U251 cells. (**E, F**) Statistical analysis of cells per field in (**C**) and (**D**). (**G**) Western blotting was used to measure the levels of epithelial and mesenchymal markers in U251 and U87 cells after TMBIM1 knockdown or overexpression. (**H**) TMBIM1 expression was positively associated with N-cadherin and SNAI1 expression and negatively correlated with E-cadherin expression in GBM tissues. Unpaired student t-test was used to measure statistical significance in control group and knockdown or overexpression group. * $P < 0.05$, ** $P < 0.01$, *** $P < 0.001$, Ctrl: Control.

of Beclin1 and LC3-II in U87 and U251 cells and decreased the level of p62. We also found that TMBIM1 knockdown decreased the protein levels of Beclin1 and LC3-II and increased that of p62 in U87 and U251 cells (Figs. 4D, S3B–3I). By TEM, we observed an obvious increase in the number of autophagosomes with the features of double-membraned vacuolar structures containing cellular components (Fig. 4E, F). Lenti-mCherry-

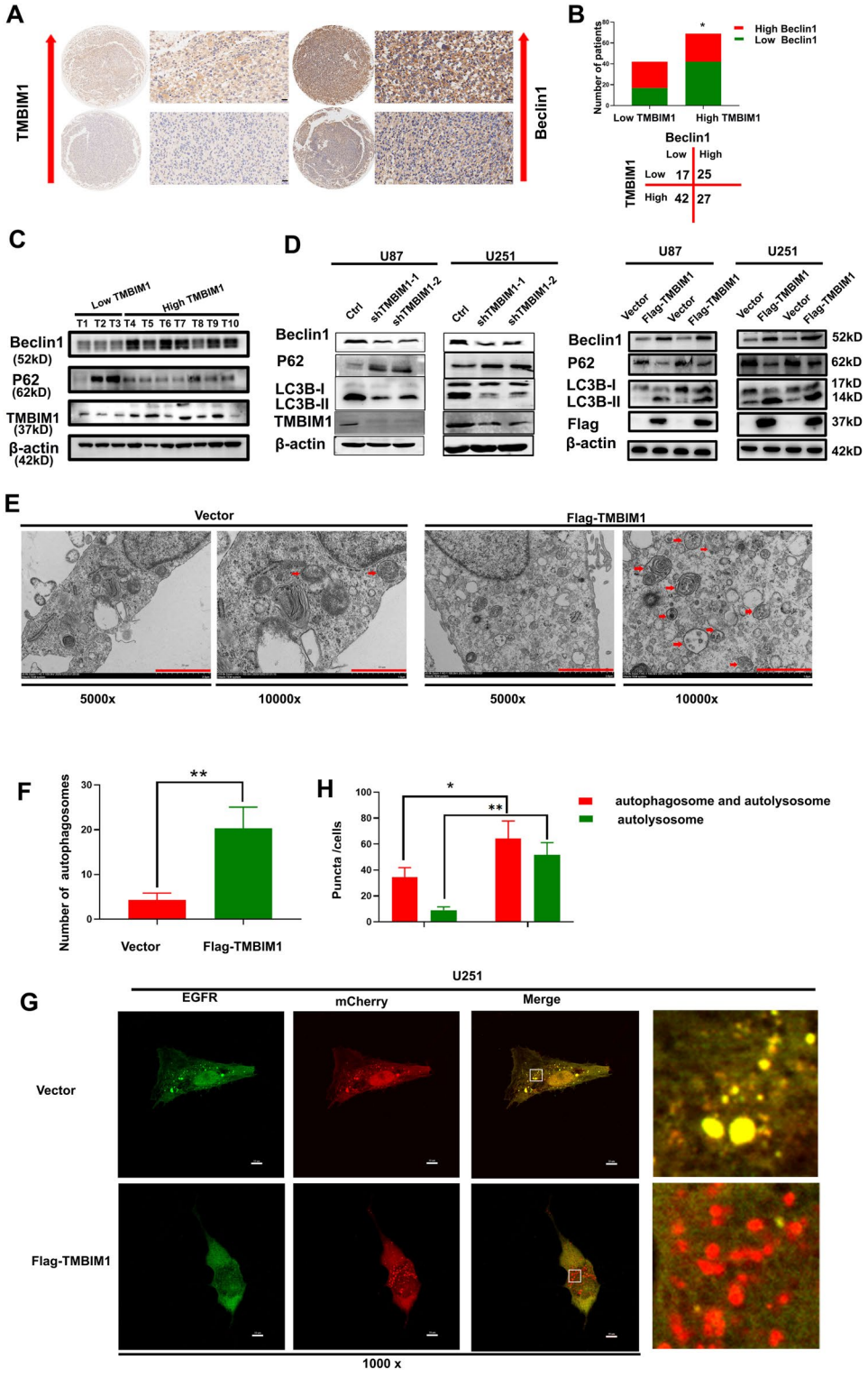

EGFP-LC3B is a lentivirus that can express the mCherry-EGFP-LC3B fusion protein and is widely used for monitoring of autophagic flux. After transfection of U251 cells with the vector or Flag-TMBIM1 plasmid, we infected these cells with EGFP-mCherry-LC3B lentivirus to investigate and monitor autophagic flux. Yellow and red puncta represent autophagosomes and autolysosomes, respectively. When autophagosomes and lysosomes fuse to form autolysosomes, the acidic environment inside the autolysosomes leads to the quenching of EGFP-derived green fluorescence, resulting in more red puncta. Therefore, a decrease in EGFP can indicate the rate of autolysosome formation. The intensity of the EGFP signal in cells transfected with the vector was similar to the mCherry signal intensity, and most of the puncta were yellow. However, in TMBIM1-overexpressing cells, only weak EGFP signals were observed, and most of the puncta were nearly red (Fig. 4G, H), indicating that autophagic flux was unobstructed. These data suggest that TMBIM1 stimulates autophagy in GBM cells.

◀**Fig. 4**. TMBIM1 stimulates autophagy in GBM cells. (**A**) Representative images of IHC staining showed that TMBIM1 expression was positively correlated with Beclin1 expression in the same tissues. Scale bars, 20 um. (**B**) The expression of TMBIM1 and Beclin1 in 111 glioma samples was analyzed. (**C**) TMBIM1 expression was positively correlated with that of Beclin1 and negatively correlated with that of P62 in GBM tissues. (**D**) Western blot analysis showed that the expression of autophagy-related proteins was upregulated or downregulated in cells with TMBIM1 overexpression or knockdown, respectively. (**E, F**) TMBIM1 overexpression increased the number of autophagosomes in U251 cells. Electron microscopy revealed typical autolysosomes (indicated by the red arrowhead). Scale bars, 20um(5000x),10um(10000x). (**G, H**) Lenti-mCherry-EGFP-LC3B lentivirus was used to monitor autophagic flux in U251 cells after transfection with the vector or Flag-TMBIM1 plasmid. Autophagosomes (yellow puncta) and autolysosomes (red puncta) in the cells were visualized by confocal microscopy. Scale bars, 10um. Unpaired student t-test was used to measure statistical significance in control group and knockdown or overexpression group. * $P < 0.05$, ** $P < 0.01$, *** $P < 0.001$.

Inhibition of autophagy reverses EMT in GBM cells

3-Methyladenine (3-MA) and chloroquine (CQ) are widely used autophagy inhibitors that exert antiautophagic effects by inhibiting class III PI3Ks and blocking the fusion of autophagosomes and lysosomes, respectively[25]. To investigate the underlying mechanism by which autophagy regulates EMT, we used 3-MA and CQ to treat GBM cells. Transwell assays showed that inhibition of autophagy by 3-MA and CQ reduced the migration and invasion of TMBIM1 overexpression and knockdown cells (Figs. 5A–D; S4A–4D). Moreover, inhibition of autophagy affected the expression of EMT-related proteins in cells with TMBIM1 knockdown or overexpression. Treatment with 3-MA and CQ enhanced E-cadherin expression and reduced the expression of Vimentin, SNAI1 and N-cadherin in U251 cells with TMBIM1 knockdown or overexpression (Figs. 5E, S4E–4F). These results revealed that suppression of autophagy reverses EMT in GBM cells.

TMBIM1 accelerates the degradation of E-cadherin through the lysosomal pathway

Previous studies have indicated that the selective degradation of specific EMT proteins seems to be the main molecular mechanism by which autophagy mediates EMT[26] . Since loss of E-cadherin expression is considered the basis of EMT, we hypothesized that TMBIM1 may mediate the EMT process in GBM by affecting the synthesis or degradation of E-cadherin. Therefore, we investigated the protein and mRNA expression of TMBIM1 after transfection of the Flag-TMBIM1 plasmid at a specific concentration and found that TMBIM1 overexpression reduced the protein level of E-cadherin but had no effect on its mRNA level (Fig. 6A–C). Therefore, we speculated that TMBIM1 reduced the protein level of E-cadherin by promoting its degradation. Cycloheximide (CHX), a protein synthesis inhibitor, was added to U251 cells, and it was shown that the expression of E-cadherin decreased after treatment with CHX for a certain time. However, the degradation rate of E-cadherin protein in TMBIM1 knockdown cells was slower, indicating that TMBIM1 knockdown can inhibit the degradation of the E-cadherin protein in GBM cells (Fig. 6D, E). The lysosomal pathway and proteasome pathway are the main pathways for protein degradation[9]. We then sought to identify the pathway of E-cadherin degradation induced by TMBIM1. Our results demonstrated that chloroquine (CQ), which inhibits the function of lysosomes, delayed the degradation of E-cadherin in TMBIM1 knockdown cells, but MG132, which inhibits the function of the proteasome, did not affect E-cadherin degradation (Fig. 6F–I). Therefore, our results revealed that TMBIM1 accelerates the degradation of E-cadherin through the lysosomal pathway.

TMBIM1 stimulates autophagy via the AMPK/mTOR/ULK1 axis in GBM cells

AMPK, a regulator of cellular and organismal metabolism, is also involved in the regulation of autophagy[27]. Phosphorylation at Thr172 is required for AMPK kinase activity[28]. In addition, Ser317 is one of the major sites of AMPK-mediated phosphorylation of ULK1[29]. Thus, we investigated whether the AMPK pathway is related to TMBIM1-induced autophagy in GBM cells. We first evaluated the levels of p-AMPKα Thr172 and p-ULK1 Ser317 in GBM tissues by Western blotting. The results showed that the levels of p-AMPKα Thr172 and p-ULK1 Ser317 were positively correlated with the TMBIM1 expression level (Figs. 7A, S5A). In addition, TMBIM1 knockdown decreased the levels of p-AMPKα Thr172 and p-ULK1 Ser317 in U87 and U251 cells and increased the level of p-mTOR Ser2448. We also found that TMBIM1 overexpression increased the levels of p-AMPKα Thr172 and p-ULK1 Ser317 and reduced the level of p-mTOR Ser2448 in U87 and U251 cells. However, TMBIM1 had no effect on the AMPK and mTOR levels (Figs. 7B, S5B–5E). These results suggested that TMBIM1 stimulates autophagy by activating AMPK pathways in GBM cells. To further confirm our hypothesis, Compound C (C C) was used to treat cells with TMBIM1 knockout/overexpression. Compound C, also called BML-275, is an effective AMPK inhibitor. Consistent with our expectations, Western blot analysis showed that autophagy was suppressed after inhibition of the AMPK pathway by Compound C (Figs. 7C, S5F–5I). Furthermore, we observed that the numbers of autophagosomes and autolysosomes in TMBIM1-overexpressing cells were decreased after Compound C treatment (Fig. 7D–G).

TMBIM1 knockdown suppresses autophagy and EMT in an intracranial xenograft model

To further investigate the effect of TMBIM1 on autophagy and EMT, we established an intracranial xenograft model. The tumor volume in TMBIM1 knockdown mice was less than that in control mice, as determined by whole-body bioluminescence imaging and hematoxylin and eosin (H&E) staining. Interestingly, the tumor volume in TMBIM1 knockdown mice was decreased after CQ treatment (Fig. 8A, C). As expected, the survival time of TMBIM1 knockdown mice was longer than that of mice in the control group. Surprisingly, the survival

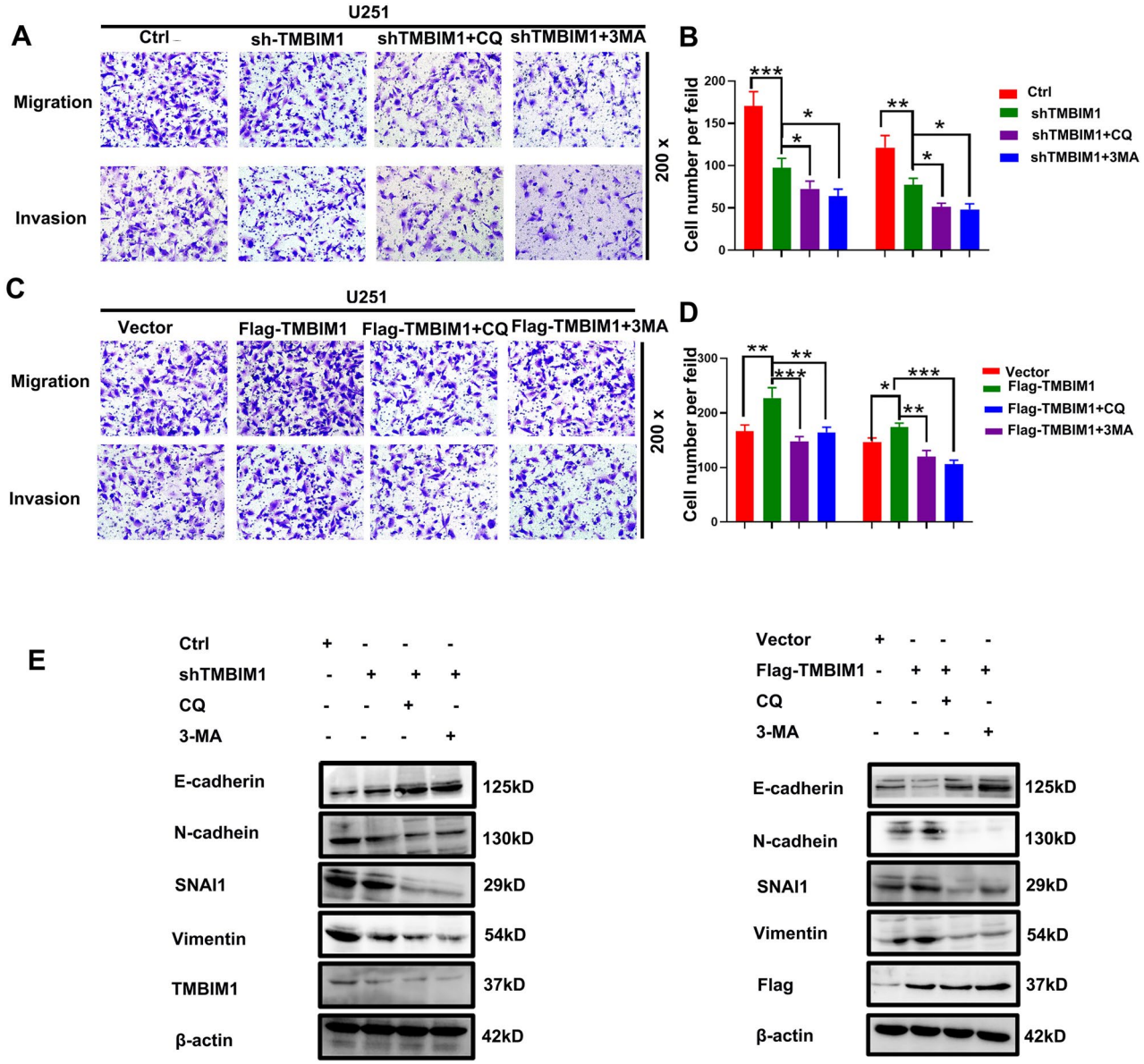

Fig. 5. Inhibition of autophagy reverses EMT in GBM cells. (**A, C**) Inhibition of autophagy by CQ and 3-MA reduced the migration and invasion of U251 cells with TMBIM1 knockdown/overexpression. (**B, D**) Statistical analysis of cells per field in (**A**) and (**C**). (**E**) Inhibition of autophagy reversed the changes in the expression of epithelial markers and mesenchymal markers in TMBIM1-overexpressing cells and further increased E-cadherin expression and decreased N-cadherin, vimentin and SNAI1 expression in TMBIM1-knockdown cells. One-way analysis of variance (ANOVA) was used measure statistical significance, and Tukey's test was used to compare differences between groups. * $P < 0.05$, ** $P < 0.01$, *** $P < 0.001$.

time of mice in the TMBIM1 knockdown group was further prolonged after CQ treatment (Fig. 8B). IHC staining showed that TMBIM1 knockdown resulted in decreased protein levels of p-AMPKα, p-ULK1 and Beclin1 and increased protein levels of p-mTOR and P62 (Figs. 8D, S6A, 6B). Moreover, TMBIM1 knockdown decreased the expression of N-cadherin, Vimentin and SNAI1 and enhanced E-cadherin expression. We also found that CQ-treated mice in the TMBIM1 knockdown group exhibited a further increase in E-cadherin expression and decreased expression of N-cadherin, Vimentin and SNAI1 (Figs. 8E, S6C, 6D), which was consistent with the in vitro results. As shown in Fig. 9, TMBIM1 functions as a lysosomal transmembrane protein to promote EMT by stimulating autophagic degradation of E-cadherin via the AMPK/mTOR/ULK1 axis in GBM cells. These results suggested that inhibition of TMBIM1-induced autophagy may be an underlying strategy for the prevention and treatment of glioma.

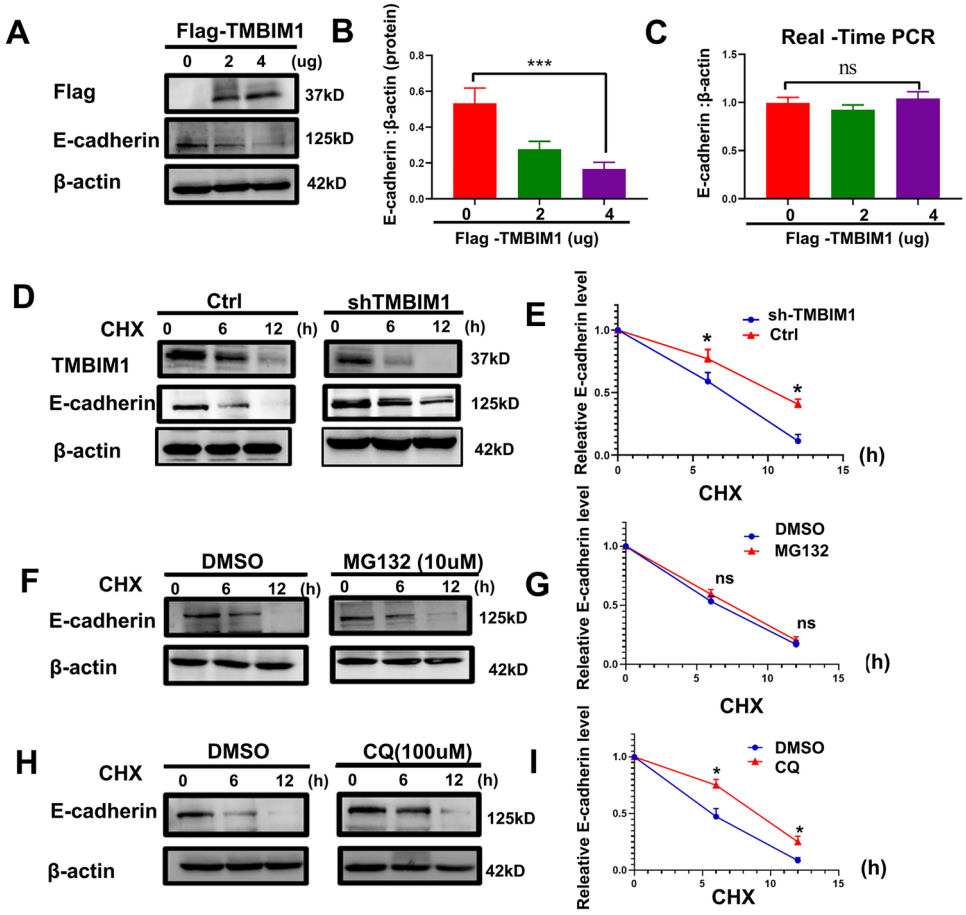

Fig. 6. TMBIM1 accelerates the degradation of E-cadherin through the lysosomal pathway. (**A–C**) U251 cells were transfected with the indicated concentrations of Flag-TMBIM1 for 48 h, and TMBIM1 overexpression was found to decrease the E-cadherin protein level but not affect the E-cadherin mRNA level. (**D–E**) U251-shTMBIM1 and control cells were treated with CHX (10 μM) for the indicated times, and TMBIM1 knockdown was found to inhibit E-cadherin protein degradation. (**F, G**) CHX (10 μM) was added to U251-shTMBIM1 cells for the indicated times after treatment with MG132 (10 μM) for 2 h. Western blot analysis suggested that TMBIM1 does not affect the proteasomal degradation of E-cadherin. (**H, I**) CHX (10 μM) was added to U251-shTMBIM1 cells for the indicated times after treatment with CQ (100 μM) for 24 h. Western blot analysis indicated that TMBIM1 accelerates the lysosomal degradation of E-cadherin. One-way analysis of variance (ANOVA) was used measure statistical significance, and Tukey's test was used to compare differences between groups. *P < 0.05, ***P < 0.001, Ctrl: Control, CHX cycloheximide; CQ chloroquine; ns, nonsignificant.

Discussion

TMBIM1 is a lysosomal transmembrane protein that inhibits adipogenesis and ameliorates obesity-related metabolic diseases by reducing the stability of peroxisome proliferator-activated receptor-γ (PPAR-γ)[16]. In addition, TMBIM1 is involved in the prevention of nonalcoholic steatohepatitis, metabolic syndrome and cardiomyopathy[15,16]. However, few studies have linked TMBIM1 with the formation and progression of human tumors. Our study showed for the first time that the expression of TMBIM1 in GBM tissues was significantly higher than that in normal brain tissues. The prognosis of GBM and LGG patients with low TMBIM1 expression was better than the prognosis of those with high TMBIM1 expression. Furthermore, TMBIM1 knockdown mice had longer survival times in the intracranial xenograft experiment. Cox regression analysis based on TCGA and CGGA datasets indicated that TMBIM1 is an independent risk factor for human glioma.

Tumor metastasis is closely related to EMT, which is a critical step in cancer progression and has been identified as a marker of advanced tumor development and poor prognosis[30]. In our research, we demonstrated that TMBIM1 induces EMT and autophagy in GBM cells. Recent research has revealed that there is a complex link between EMT and autophagy. Increasing evidence indicates that autophagy plays a dual role in the regulation of EMT[6]. It has been reported that deficiency of autophagy inhibits TWIST1 degradation through autophagosomes and promotes EMT, tumor growth and metastasis in mice[31]. Sahib Zada found that autophagic degradation of SNAI1 inhibited EMT and metastasis in HeLa and H1299 cells[32] . Myriam Catalano reported that autophagy reversed EMT in glioblastoma cells and inhibited cell invasion and migration[33]. These studies indicate that autophagy plays a negative role in EMT. However, autophagy seems to be an active regulator of EMT. A recent study indicated that SPHK1 induces EMT by promoting autophagic degradation of E-cadherin in HepG2 cells[9].

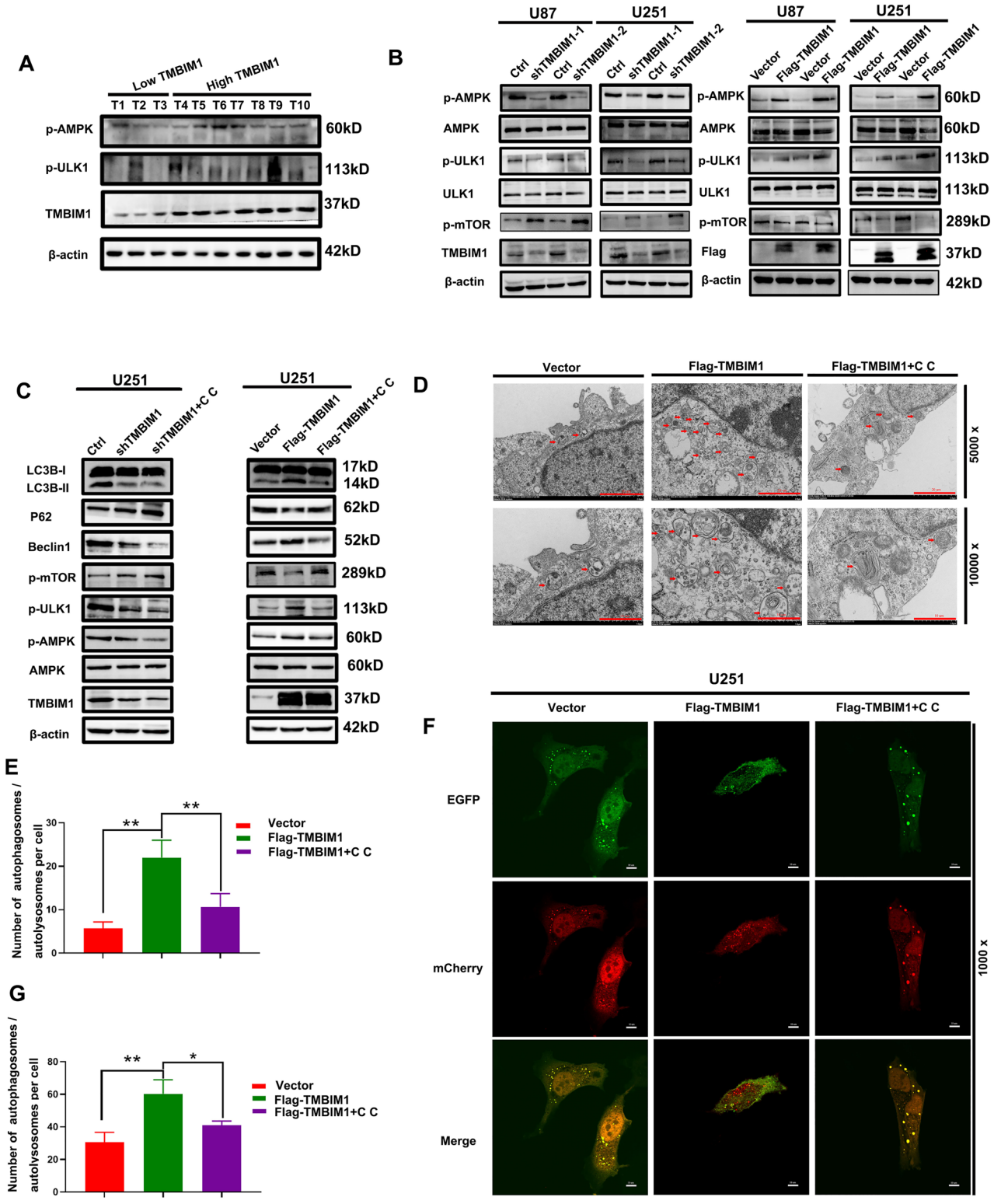

Similarly, another study revealed that Sirtuin-1 (SIRT1) accelerates tumor metastasis by stimulating autophagic degradation of E-cadherin[34]. Therefore, we speculated that the function of autophagy in regulating EMT mainly depends on the tissue/cell type and tumor development stage. E-cadherin is a key protein involved in EMT, and E-cadherin loss is considered the basis of EMT, and its expression is closely linked to EMT and tumor metastasis[8]. Hong L and Ting Sun reported that E-cadherin is degraded via the lysosomal pathway[9,34]. Su Mi demonstrated that autophagy is involved in the regulation of the endocytic lysosomal pathway[35]. Hongliang Li identifiedTMBIM1 as a previously unknown regulator of the multivesicular body (MVB)-lysosomal pathway and found that it prevents nonalcoholic steatohepatitis (NASH) in mice and monkeys by promoting lysosomal degradation of TLR4[15]. Therefore, we speculate that there may be an important connection between TMBIM1-related lysosomal pathways and E-cadherin proteins. In our study, we demonstrated that TMBIM1 reduced the

◂**Fig. 7**. TMBIM1 stimulates autophagy by mediating AMPK/mTOR/ULK1 signaling in GBM cells. (**A**) The TMBIM1 expression level was positively correlated with the p-AMPK and p-ULK1 levels in human GBM tissues. (**B**) Western blot analysis of the protein levels of p-AMPKα Thr172, p-ULK1 Ser317, p-mTOR Ser2448, AMPK and ULK1 in GBM cells with TMBIM1 knockdown/overexpression. (**C**) Inhibition of the AMPK pathway was induced by Compound C treatment, and western blotting was used to measure the levels of autophagy-related proteins and key proteins of the AMPK pathway. (**D**, **E**) Electron microscopy revealed the number of autolysosomes after inhibition of the AMPK pathway with Compound C. Scale bars, 20 um (5000x),10 um (10000x). (**F, G**) Confocal microscopy observation revealed that the numbers of autophagosomes (yellow puncta) and autolysosomes (red puncta) were decreased after Compound C treatment in TMBIM1-overexpressing U251 cells. One-way analysis of variance (ANOVA) was used measure statistical significance, and Tukey's test was used to compare differences between groups. Scale bars, 10um. * $P < 0.05$, ** $P < 0.01$, C C: Compound C.

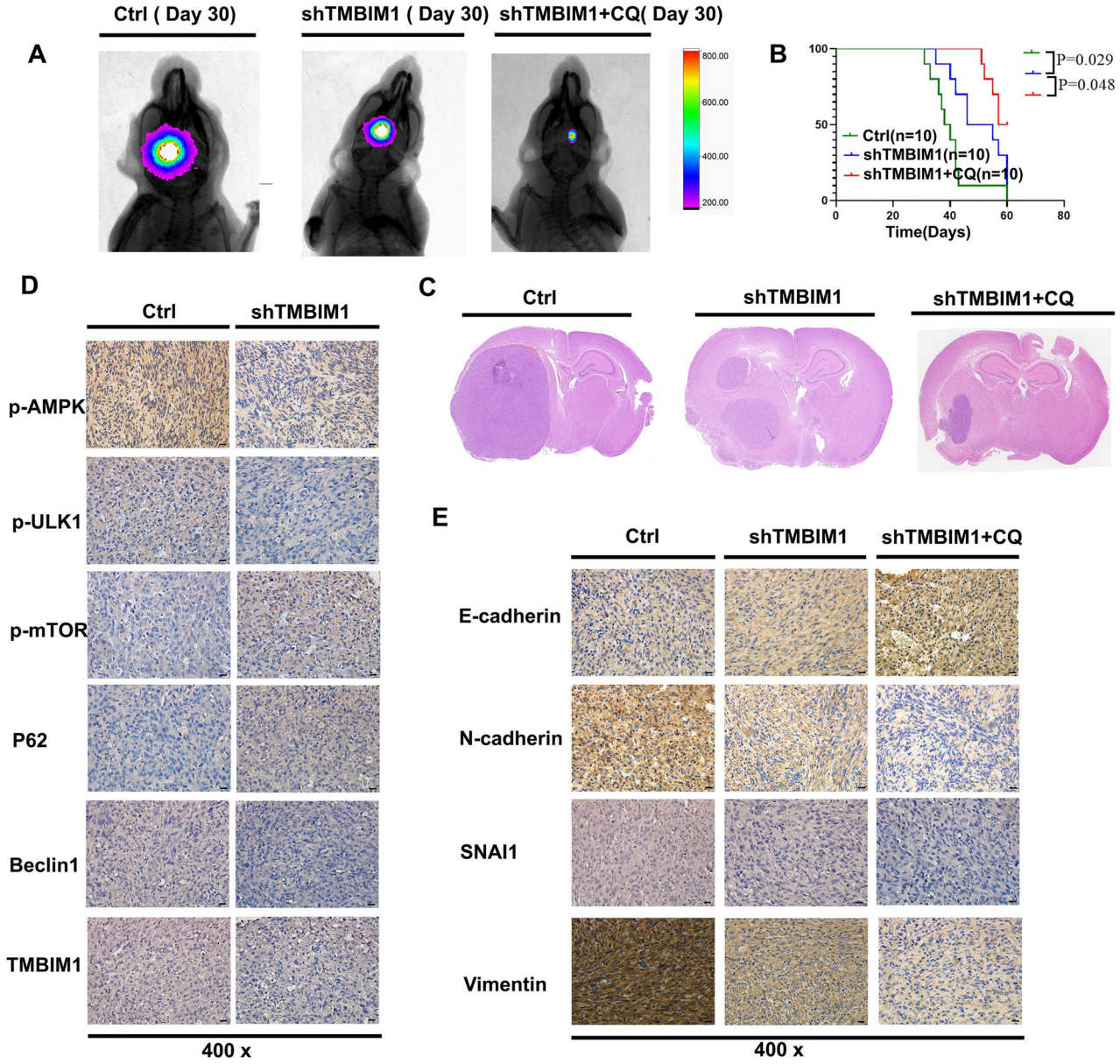

Fig. 8. TMBIM1 knockdown suppresses autophagy and EMT in an intracranial xenograft model. (**A**) In vivo bioluminescence imaging of nude mice 30 days after cell inoculation. (**B**) Mouse survival was shown by Kaplan–Meier analysis. The log-rank test was used to measure survival differences. (**C**) HE staining. (**D**) IHC staining of p-AMPK (Thr172), p-ULK1 (Ser317), p-mTOR (Ser2448), Beclin1, P62 and TMBIM1. Scale bars, 20 um. (**E**) IHC staining of E-cadherin, N-cadherin, Vimentin and SNAI1. Scale bars, 20 um.

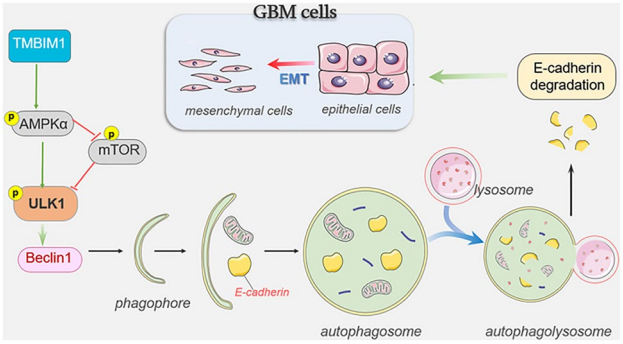

Fig. 9. Schematic diagram of the mechanism by which TMBIM1 mediates the autophagic degradation of E-cadherin, which stimulates EMT in GBM cells.

protein level of E-cadherin but did not reduce the mRNA level of E-cadherin, and inhibition of autophagy by CQ and 3-MA reversed EMT and impaired the migration and invasion of GBM cells. Subsequently confirmed that suppression of autophagy by CQ delayed lysosomal degradation of E-cadherin. In addition, it has been found that e-cadherin is delivered to the autophagosome after autophagy activation and is degraded by p62. Histone deacetylases SIRT1 and SIRT6 promote the metastasis potential of melanoma and hepatocellular cancer cells, respectively, by deacetylating Beclin-1 and accelerating the autophagy degradation of e-cadherin[36]. These results suggest that TMBIM1 promotes autophagic degradation of E-cadherin, which may be associated with Beclin1 and P62. In summary, our study revealed that TMBIM1 promotes EMT in GBM by stimulating autophagy-linked lysosomal degradation of E-cadherin.

AMPK is an important regulator involved in energy metabolism, cell growth and autophagy in cells. Previous findings have shown that AMPK mediates autophagy by regulating the phosphorylation of ULK1, and the formation of the isolation membrane by activated ULK1 is considered to be the first step of autophagosome formation[37]. AMPK-mediated activation of ULK1 mainly involves two mechanisms, one of which is direct activation of ULK1 by AMPK-mediated phosphorylation at Ser317, Ser777 and Ser555. The other is indirect activation by suppression of mTOR phosphorylation[29]. In this study, we found that the protein levels of p-AMPK and p-ULK1 in the TMBIM1 overexpression group were increased but the level of p-mTOR was dramatically decreased both in vivo and in vitro. In addition, our data demonstrated that autophagy was inhibited by suppressing the AMPK pathway with Compound C in cells with TMBIM1 knockdown or overexpression. These results indicated that TMBIM1 mediates autophagy via the AMPK/mTOR/ULK1 signaling pathway.

In conclusion, this study suggests that TMBIM1 promotes EMT by accelerating autophagic degradation of E-cadherin in GBM. TMBIM1 is a novel prognostic factor and therapeutic target in GBM. Our findings reveal that blocking TMBIM1 activity to suppress autophagy may be a fundamental strategy for the prevention and treatment of GBM[38].

Data availability

All data generated or analyzed during this study are included in this published article and its supplementary information files.

Received: 28 August 2024; Accepted: 7 May 2025
Published online: 20 May 2025

References

1. Reifenberger, G., Wirsching, H. G., Knobbe-Thomsen, C. B. & Weller, M. Advances in the molecular genetics of gliomas—implications for classification and therapy. *Nat. Rev. Clin. Oncol.* **14**(7), 434–452 (2017).
2. Gusyatiner, O. & Hegi, M. E. Glioma epigenetics: from subclassification to novel treatment options. *Semin. Cancer Biol.* **51**, 50–58 (2018).
3. Bilmin, K., Kujawska, T. & Grieb, P. Sonodynamic therapy for gliomas. Perspectives and prospects of selective sonosensitization of glioma cells. *Cells* **8**, 11 (2019).
4. Yu, F. et al. SPOCK1 is upregulated in recurrent glioblastoma and contributes to metastasis and Temozolomide resistance. *Cell Prolif.* **49**(2), 195–206 (2016).
5. Colella, B., Faienza, F. & Di Bartolomeo, S. EMT regulation by autophagy: a new perspective in glioblastoma biology. *Cancers* **11**, 3 (2019).
6. Chen, H. T. et al. Crosstalk between autophagy and epithelial-mesenchymal transition and its application in cancer therapy. *Mol. Cancer* **18**(1), 101 (2019).
7. Meena, D. & Jha, S. Autophagy in glioblastoma: a mechanistic perspective. *Int. J. Cancer* **155**(4), 605–617 (2024).
8. Babaei, G., Aziz, S. G., Jaghi, N. Z. Z. EMT, cancer stem cells and autophagy; the three main axes of metastasis. *Biomed. Pharmacother. Biomed. Pharmacother.* **133**, 110909 (2021).
9. Liu, H., Ma, Y., He, H. W., Zhao, W. L. & Shao, R. G. SPHK1 (sphingosine kinase 1) induces epithelial-mesenchymal transition by promoting the autophagy-linked lysosomal degradation of CDH1/E-cadherin in hepatoma cells. *Autophagy* **13**(5), 900–913 (2017).
10. Liu, X. et al. Regulation of FN1 degradation by the p62/SQSTM1-dependent autophagy-lysosome pathway in HNSCC. *Int. J. Oral Sci.* **12**(1), 34 (2020).

11. Li, H. et al. HERC3-mediated SMAD7 ubiquitination degradation promotes autophagy-induced EMT and chemoresistance in glioblastoma. *Clin. Cancer Res.* **25**(12), 3602–3616 (2019).
12. Zhao, H. et al. RECS1 deficiency in mice induces susceptibility to cystic medial degeneration. *Genes Genet. Syst.* **81**(1), 41–50 (2006).
13. Guo, G. et al. Ion and pH sensitivity of a TMBIM Ca(2+) channel. *Structure (Lond., Engl. 1993)* **27**(6), 1013–21.e3 (2019).
14. Zhang, J. et al. Genetic variant of TMBIM1 is associated with the susceptibility of colorectal cancer in the Chinese population. *Clin. Res. Hepatol. Gastroenterol.* **43**(3), 324–329 (2019).
15. Zhao, G. N. et al. Tmbim1 is a multivesicular body regulator that protects against non-alcoholic fatty liver disease in mice and monkeys by targeting the lysosomal degradation of Tlr4. *Nat. Med.* **23**(6), 742–752 (2017).
16. Zhao, G. N. et al. TMBIM1 is an inhibitor of adipogenesis and its depletion promotes adipocyte hyperplasia and improves obesity-related metabolic disease. *Cell Metab.* **33**(8), 1640–54.e8 (2021).
17. Bowman, R. L., Wang, Q., Carro, A., Verhaak, R. G. & Squatrito, M. GlioVis data portal for visualization and analysis of brain tumor expression datasets. *Neuro Oncol.* **19**(1), 139–141 (2017).
18. Liu, J. et al. Gasdermin D is a novel prognostic biomarker and relates to TMZ response in glioblastoma. *Cancers* **13**, 22 (2021).
19. Han, M. Z. et al. TAGLN2 is a candidate prognostic biomarker promoting tumorigenesis in human gliomas. *J. Exp. Clin. Cancer Res.* **36**(1), 155 (2017).
20. Pyo, J. O., Nah, J. & Jung, Y. K. Molecules and their functions in autophagy. *Exp. Mol. Med.* **44**(2), 73–80 (2012).
21. Islam, M. A., Sooro, M. A. & Zhang, P. Autophagic regulation of p62 is critical for cancer therapy. *Int. J. Mol. Sci.* **19**, 5 (2018).
22. Li, X., He, S. & Ma, B. Autophagy and autophagy-related proteins in cancer. *Mol. Cancer* **19**(1), 12 (2020).
23. Vishnupriya, S., Priya Dharshini, L. C., Sakthivel, K. M. & Rasmi, R. R. Autophagy markers as mediators of lung injury-implication for therapeutic intervention. *Life Sci.* **260**, 118308 (2020).
24. Panda, S. P. & Singh, V. The dysregulated MAD in Mad: a neuro-theranostic approach through the induction of autophagic biomarkers LC3B-II and ATG. *Mol. Neurobiol.* **60**(9), 5214–5236 (2023).
25. Wang, S., Livingston, M. J., Su, Y. & Dong, Z. Reciprocal regulation of cilia and autophagy via the MTOR and proteasome pathways. *Autophagy* **11**(4), 607–616 (2015).
26. Gugnoni, M., Sancisi, V., Manzotti, G., Gandolfi, G. & Ciarrocchi, A. Autophagy and epithelial-mesenchymal transition: an intricate interplay in cancer. *Cell Death Dis.* **7**(12), e2520 (2016).
27. Mihaylova, M. M. & Shaw, R. J. The AMPK signalling pathway coordinates cell growth, autophagy and metabolism. *Nat. Cell Biol.* **13**(9), 1016–1023 (2011).
28. Kim, J., Kundu, M., Viollet, B. & Guan, K. L. AMPK and mTOR regulate autophagy through direct phosphorylation of Ulk1. *Nat. Cell Biol.* **13**(2), 132–141 (2011).
29. Paquette, M., El-Houjeiri, L. & Pause, A. mTOR pathways in cancer and autophagy. *Cancers* **10**, 1 (2018).
30. Su, Z., Yang, Z., Xu, Y., Chen, Y. & Yu, Q. Apoptosis, autophagy, necroptosis, and cancer metastasis. *Mol. Cancer* **14**, 48 (2015).
31. Qiang, L. & He, Y. Y. Autophagy deficiency stabilizes TWIST1 to promote epithelial-mesenchymal transition. *Autophagy* **10**(10), 1864–1865 (2014).
32. Zada, S., Hwang, J. S., Ahmed, M., Lai, T. H., Pham, T. M. & Kim, D. R. Control of the epithelial-to-mesenchymal transition and cancer metastasis by autophagy-dependent SNAI1 degradation. *Cells* **8**, 2 (2019).
33. Catalano, M. et al. Autophagy induction impairs migration and invasion by reversing EMT in glioblastoma cells. *Mol. Oncol.* **9**(8), 1612–1625 (2015).
34. Sun, T., Jiao, L., Wang, Y., Yu, Y. & Ming, L. SIRT1 induces epithelial-mesenchymal transition by promoting autophagic degradation of E-cadherin in melanoma cells. *Cell Death Dis.* **9**(2), 136 (2018).
35. Mi, S. et al. Blocking IL-17A promotes the resolution of pulmonary inflammation and fibrosis via TGF-beta1-dependent and -independent mechanisms. *J. Immunol. (Baltimore, Md : 1950)* **187** (6), 3003–3014 (2011).
36. Santarosa, M. & Maestro, R. The autophagic route of E-cadherin and cell adhesion molecules in cancer progression. *Cancers* **13**, 24 (2021).
37. Wang, L. et al. Chikusetsu saponin IVa attenuates isoprenaline-induced myocardial fibrosis in mice through activation autophagy mediated by AMPK/mTOR/ULK1 signaling. *Phytomedicine* **58**, 152764 (2019).
38. Lun Gao, Junhui Liu, Shenqi Zhang et al. TMBIM1 promotes EMT by stimulating autophagic degradation of E-cadherin via AMPK/mTOR/ULK1 axis in human gliomas, PREPRINT (Version 3) available at Research Square. https://doi.org/10.21203/rs.3.rs-1403508/v3. (2022).

Author contributions

LG, J-HL, GD and Q-XC conceived and designed the study. LG, J-HL, YL, J-AY and LW performed the experiments. LG, ZY, J-AY, J-YC and S-AT analyzed the data. LG, GD, QC and J-HL wrote the manuscript. All authors contributed to the article and approved the submitted version.

Funding

This work was supported by the National Natural Science Foundation of China (Nos. 82072764, 82001311, 81971158, 82203163, and 81671306), Wuhan Science and Technology Plan Project (2019020701011470) and Fundamental Research Funds for the Central Universities (2042021kf0090).

Competing interests

The authors declare no competing interests.

Consent for publication

All the listed authors participated in the study and approved the submitted manuscript.

Ethic statement

This study was approved by the Ethics Committee of the Renmin Hospital of Wuhan University [approval number: 2012LKSZ (010) H], and all procedures were conducted in accordance with the Helsinki Declaration and all the patients signed the informed consent form. Animal Studies: This study was approved by the Animal Ethics Committee of Renmin Hospital of Wuhan University [approval number: WDRM 20201111], and all methods were carried out in accordance with ARRIVE guidelines. All methods were performed in accordance with the relevant guidelines and regulations.

Additional information

Supplementary Information The online version contains supplementary material available at https://doi.org/10.1038/s41598-025-01699-4.

Correspondence and requests for materials should be addressed to G.D., Q.C. or Q.C.

Reprints and permissions information is available at www.nature.com/reprints.

Publisher's note Springer Nature remains neutral with regard to jurisdictional claims in published maps and institutional affiliations.